WOOD AND FIBER

JOURNAL OF THE SOCIETY OF WOOD SCIENCE AND TECHNOLOGY

VOLUME 2 SUMMER 1970 NUMBER 2

NEW MODELS IN CELL-WALL MECHANICS[1]

Richard E. Mark[2]
Department of Forestry, University of Kentucky, Lexington, Ky. 40506

and

Peter P. Gillis
Department of Metallurgical Engineering and Materials Science
University of Kentucky, Lexington, Ky. 40506

ABSTRACT

A comparison is made of the mechanical behavior of fiber cell-wall models with complete shear restraint and the earlier model of Mark in which shear restraint was assumed in the case of the S1 layer only. Literature review and experimental work indicate that for different circumstances, different models may be more appropriate. A further modification of the general analytical approach is offered—a "two-wall" analysis that allows for the general existence of different transverse strains in radial and tangential walls, respectively. A more refined calculation of the elastic constants of each cell-wall layer is also employed. The effect of certain cell-wall parameters on stress and strain distribution is explored. New experimental work on the torsional behavior of wood fibers is presented in the light of the theoretical models for cell walls.

INTRODUCTION

With the publication of the second "complete shear restraint model" for mechanical behavior of wood fiber cell walls (Schniewind and Barrett 1969), a new and significant phase of study in cell-wall mechanics has begun. Schniewind and Barrett have made several important contributions: (a) They have found several errors and made improvements in the detailed stress distribution analysis in Chapter 10 of "Cell Wall Mechanics of Tracheids" (Mark 1967). (b) They have offered an alternative explanation to the repeated experimental observation (Davies 1968; Grozdits and Ifju 1969; Keith and Côté 1968; Kórán 1967; Mark 1967) that failure in wood cell walls occurs within or at the boundary of the S1 layer. (c) They have developed a model for the behavior of fibers in wood assuming that the multiple wall layers of adjacent cells restrain each other from twisting so completely that stresses parallel to the grain will cause no shear strain in the wall layers of the fibers. Additionally, Schniewind (1970) has examined the internal stress distributions for a hypothetical series of cell types with the complete shear restraint model.

THE SINGLE FIBER MODEL OF MARK

Let us consider first the theoretical questions that have been raised by Schniewind

[1] The investigation reported in this paper (No. 69-8-166) is in connection with a project of the Kentucky Agricultural Experiment Station and is published with the approval of the Director.

[2] Present address: Empire State Paper Research Institute, State University of New York College of Forestry, Syracuse, New York 13210

and Barrett concerning the layered composite model used by Mark (1967), which provided for complete shear restraint only in the S1 layer. Mark's model may be described as a "single fiber" model.

Schniewind and Barrett found one fundamental error in that part of the computation by Mark for stresses in the two S1 plies (S and Z). This was corrected by them, together with Mark's equation 10–20 that made that portion of the analysis more consistent with the assumptions used for the remainder.

Mark treated the cell wall as a series of individual layers having different geometrical characteristics as well as physical and chemical differences. The elastic properties of these layers were calculated by the method of Greszczuk (1964). Each layer was characterized by the volume fractions of structural carbohydrate framework (principally cellulose) and matrix material (the remaining substances in the layer) and the angle at which its microfibrils lie with respect to the cell axis. Parallelism of the microfibrils was assumed. In the case of the S1 layer, the S and Z counter-rotating helices therein were modeled as a two-ply laminate balanced with respect to the direction of the fiber axis. The composite elastic properties were found by requiring equal in-plane strains under load and assuming plane stress. From the overall strains corresponding to a given set of tractions, the matrix and reinforcement stresses were then calculated for each layer of the cell wall.

THE COMPLETE SHEAR RESTRAINT MODEL OF CAVE

Subsequently Cave (1968, 1969) analyzed the elastic properties of the cell wall from a somewhat different point of view. He simplified the wall to a single layer having a given composition and a characteristic filament winding angle, but he brought in two novel features. The first was a recognition that adjacent walls of neighboring cells having the same characteristic angle would be crisscrossed and thus would form a two-ply balanced layer. This concept allows an important simplification to be made in the elastic analysis, viz, that direct axial loading of fibers will not cause them to twist. In other words, there is no coupling between shear and extension with reference to the principal directions of elasticity of the two-ply balanced laminate.

Thus Cave was the first to introduce a cell-wall model with complete shear restraint. In addition, Cave generalized his model by assuming that the characteristic layer angle was not the direction of each microfibril but the average according to some postulated distribution function. He went on to calculate numerical results based upon a Gaussian distribution, which he then compared to experimental data from specimens of *Pinus radiata* determined to have various average S2 microfibril orientations.

COMPLETE SHEAR RESTRAINT MODEL OF SCHNIEWIND AND BARRETT

Schniewind and Barrett (1969) have concluded that no twisting of the fibers in a block of wood can occur because adjacent fiber walls, which would have to undergo opposing circumferential displacements if the fibers did twist, are firmly cemented together by the middle lamella. Their model consists of the combined layers of neighboring cell walls, the layers on one side of the middle lamella counterbalancing the corresponding layers on the other side so as to form a multi-ply balanced laminate. Conceptually, the model is similar to that of Cave (1968), but it takes the actual layered structure of the cell wall into account.

They assumed that the tendency for shear distortion in a given layer in response to an axial load was exactly balanced by the tendency of the corresponding layer of the adjacent wall towards a shear distortion of the opposite sign. Thus, no shear coupling occurs, and all layers are balanced in pairs, achieving complete shear restraint. The "single fiber" model employed by Mark (1967) does allow torsional distortion because a single cell does not have a mechanically symmetric wall structure. Schniewind

and Barrett have compared the mechanical behavior of the fiber tissue studied by Mark according to his stress analysis (corrected as mentioned earlier), which has shear restraint only in the S1 layer, with an analysis according to their complete shear restraint model. Subsequently, Schniewind (1970) calculated layer stresses for a series of hypothetical cells using this same model.

We wish to evaluate these concepts in terms of the applicability of the complete shear restraint model to solid wood (i.e. Does the model accurately describe the theoretical and experimental mechanical behavior of this material?) The evidence to be presented indicates that a negative response is in order. A corollary question, which will be dealt with further along in the paper, is "Is the single fiber model reasonable for the behavior of single fibers?"

Balashov et al. (1957) subjected xylem fiber bundles of sisal leaf (*Agave sisalana*) to tension, causing stretching of the bundles in strain increments up to 20%. At 5% axial strain, changes on the order of 3 degrees in the S2 angles of the fibers in the bundle were measured by X-ray diffraction, with tests being conducted on both wet and dry fiber bundles.[3] The extension and change in microfibrillar orientation were related to each other in the linear manner that would be predicted for a distended ideal spring model, (one in which length change takes place only by change in pitch angle, and without elongation or extension of the individual filament). For both wet and dry fibers, there was a pronounced tendency for the fibers to recover towards their original length after up to 3 to 5% elongation. The authors concluded that microfibrils must slip past each other during elongation, but that changes in microfibrillar orientation were "of reversible character." They calculated a value of the slip between adjacent microfibrils that would be permissible without breakdown of the fiber structure.

[3] In both cases the bundles had been removed intact from the sisal leaves, without separation of the fibers from each other, although some lignin was removed.

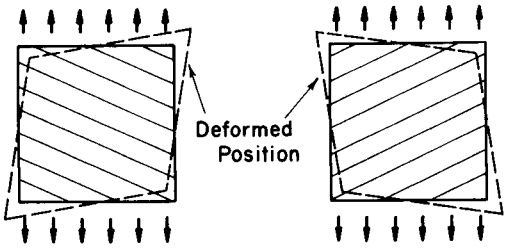

FIG. 1. Orthotropic plates with reinforcement at an angle to the edges undergoing independent shear deformation in response to axial tension (Mark 1967, p. 235).

Although Balashov and his coworkers regarded the microfibrils as ideal springs in their interpretation of these results, other analyses (Hearle 1963; Cowdrey and Preston 1966) have included contributions to strain based on microfibril stretching as well as springlike deformation. Accordingly, there may or may not be relative movement of the microfibrils in adjacent layers in cell walls. When cells have layers with different helical filament winding angles, uniform cell elongation that causes S2 angle changes, as in the experiments mentioned above, could result in relative displacements between S2 and S1, S2 and S3, etc. When this occurs, the state of strain in the individual layers would be more analogous to Fig. 1 than to Fig. 2.

Thus, it is not unequivocally correct to postulate the absence of external torsional displacements of entire cells as a sufficient

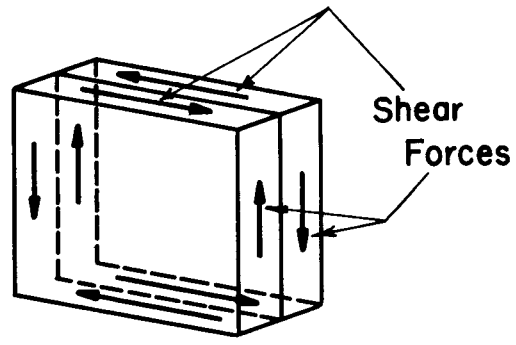

FIG. 2. Theoretical zero shear distortion of a balanced laminate when equal and opposite shear stresses are generated (Mark 1967, p. 235).

justification for assuming complete shear restraint within. The shear strains that may occur within internal layers during microfibril reorientation can be independent of twist in the entire cell.

There is also the actual possibility of some twisting or other relative movement of fibers, particularly in the case of wet wood. The middle lamella is not inherently a very stiff structure, particularly in the wet condition, because it contains a high proportion of pectic substances. Were it not for lignification, wood would not be a very coherent material. It is, after all, by apical intrusion and other forms of sliding growth (Esau 1960, pp. 60–62, 117–121) that cambial initials enlarge and mature into prosenchymatous tissue in xylem. During this growth stage, developing tracheids, fibers, and vessel elements slide upon one another and intrude between each other along the middle lamella as they elongate and grow in diameter. Therefore, the possibility cannot be excluded that the middle lamella retains some of its plastic properties. In fact, some technological processes such as bending depend on further middle lamella plasticization by steam or hot water.

Other reservations concerning the assumption of complete shear restraint include:

a. In every piece of wood there are large areas of cell-wall substance that are not correctly positioned fully to exercise mutual restraint to shear deformation upon each other (at pits, corners, intercellular spaces, along rays, etc.).
b. There is a progressive change in filament winding angles, particularly in S2, across each annual ring and from ring to ring. Commonly, within-ring changes occur in the S2 angle from *ca.* 35° in springwood to *ca.* 15° in late summerwood. In general then, the helices cannot be exactly counterbalancing between adjacent walls.
c. When large internal stresses develop, as in drying, wood in large dimensions will twist extensively, which may indicate that the fibers therein do not restrain each other fully. Of course, such twisting may also be caused by changes in grain direction or other inhomogeneity in the wood.

Lastly, there is a physical problem caused by the fact that layers that "balance" each other are neither contiguous nor truly symmetrical through the thickness (although they are symmetric with respect to the fiber axis). The asymmetry factor is serious even in thin-walled laminates and may be accentuated in the case of thick walls. It has been shown theoretically that there is a coupling between shear strain and axial tension and between bending and tension in anisotropic laminates even when the governing equations are linearized (Smith 1953, Reissner and Stavsky 1961, Whitney and Halpin 1968, Whitney 1969, and Whitney and Leissa 1969). This coupling phenomenon has now been demonstrated experimentally (Ashton et al. 1969, pp. 36–45, 98–106) for orthotropic laminates and will have to be taken into account as further refinements are made in the mechanical models for cell walls.

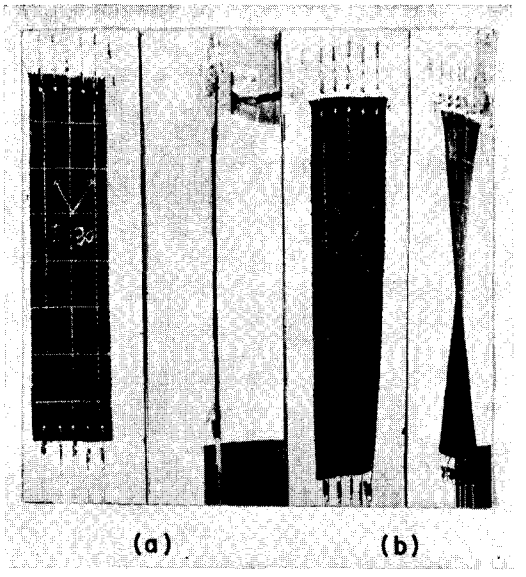

FIG. 3. Coupling between bending and stretching of a balanced two-ply laminate, (a) before test; (b) under uniaxial tension. From Ashton et al. (1969).

Figure 3 shows a two-layer strip fabricated of orthotropic layers of nylon-reinforced rubber under a tensile load. This tensile specimen is free to rotate, and thus only the axial stress resultant N_x is nonzero, while the transverse and shear stress resultants N_y and N_{xy} and all of the moment resultants are zero. The two layers are balanced with respect to the axial direction of the strip and therefore would be expected to extend without twisting or bending on the basis of simple orthotropic theory. As shown in Fig. 3, however, the strip twists under the tensile load. This effect is caused by the tendency for the two layers to exhibit equal and opposite shear deformations because of their different orientations with respect to the direction of loading. The following relation from Ashton et al. (1969, p. 38) shows the shear coupling term in addition to the normal stress resultants

$$N_x = A_{11}e_x + A_{12}e_y + B_{16}k_{xy} ,$$

where

A_{11}, A_{12} and B_{16} are elastic stiffness constants obtained through a transformation of the generalized Hooke's law for orthotropic materials;

e_x, e_y are axial and transverse strains respectively;

k_{xy} is the inverse rate of change of the slope for deflection in the laminate thickness direction under the condition that displacements are small.

Similar phenomena have been demonstrated in flexure studies on composite plates. As Fig. 4 shows, the orthotropic elasticity solution for a plate composed of a two-ply balanced laminate loaded transversely would indicate deflection according to the lower curve. But when the interlaminar coupling terms are taken into account, the very different behavior shown by the upper curve is predicted. Careful experimental work has confirmed that this type of predicted behavior does in fact occur. A two-ply plate is not sufficiently symmetrical about its own middle plane to allow neglect of the coupling phenomenon.

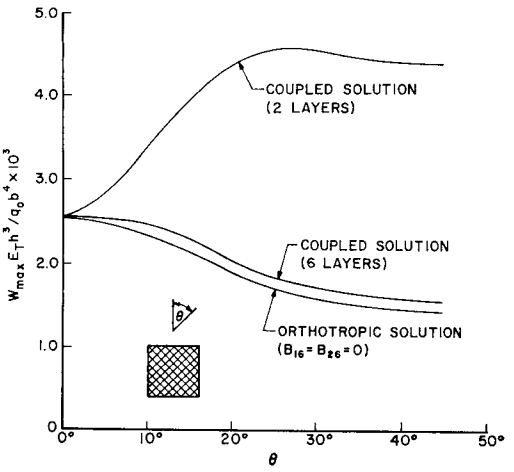

FIG. 4. Maximum deflection of square angle-ply composite plate loaded in the thickness direction. From Whitney and Leissa (1969).

This effect diminishes when four-ply, six-ply, etc. laminates are employed, and eventually the orthotropic solution is approximated when more than six plies are present in the balanced laminate (e.g. eight-ply laminates, where there are two sets of balanced laminates *on either side* of the bisector axis running in the middle plane of the plate).

When an element is taken through a double cell wall of two adjacent cells, the two-ply effect as described above is accentuated, because only the thin S1 layers on either side of the middle lamella are symmetric. Both the S2 and S3 layers are unsymmetric with respect to an axis through the middle lamella parallel to the fiber axis. Considered as a plate, such an element would have a lower bending and twisting stiffness than predicted by simple orthotropic theory; if the fiber is considered as a laminated anisotropic tube, the shear coupling terms will account for twisting of the tube in response to axial tension as shown in Fig. 5. The physical separation (noncontiguousness) of the balancing pairs of S2 and S3 layers makes the problem more pronounced and may be a major underlying reason for the warping and twisting of drying lumber. Some of the newer ap-

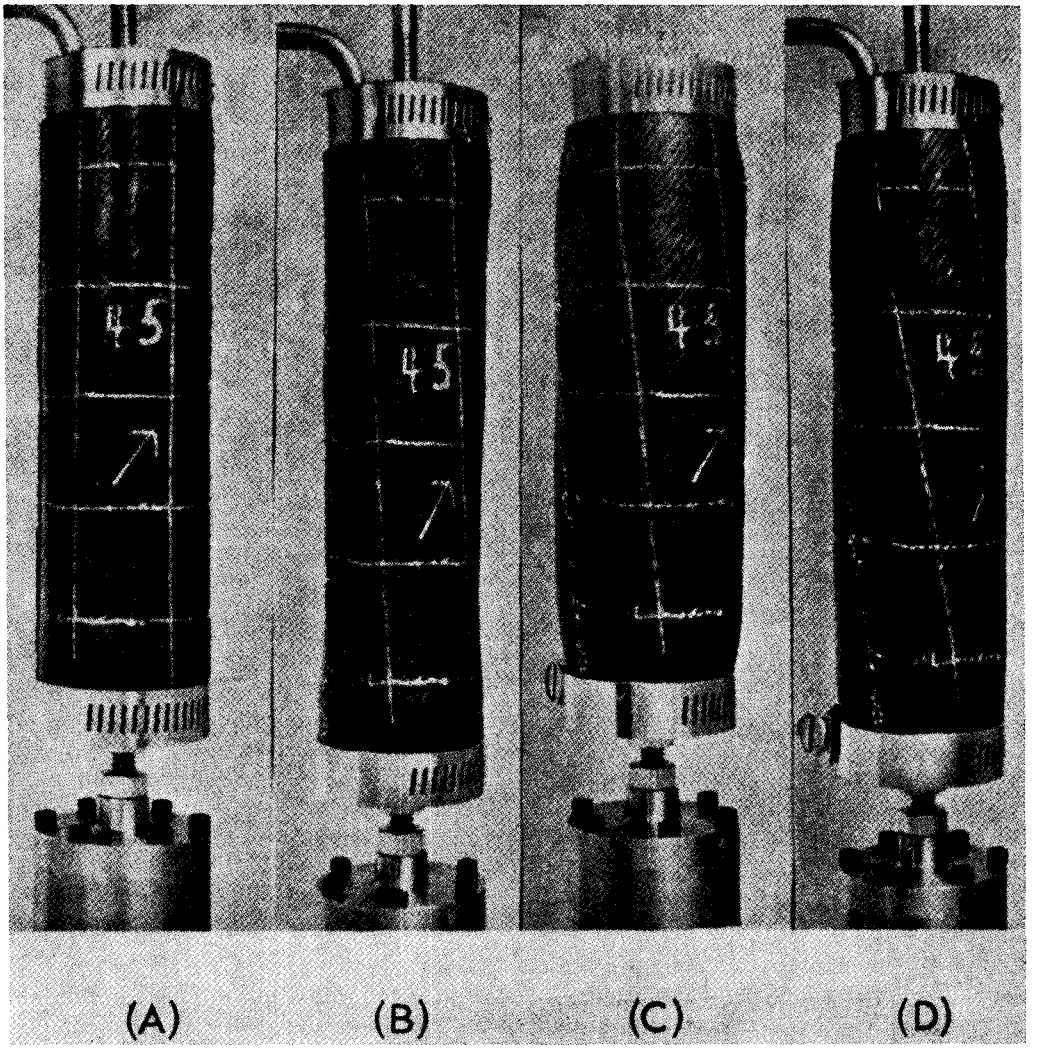

FIG. 5. Anisotropic helically-reinforced thin-walled tube illustrating twisting under tensile stress due to shear coupling. (A) Undeformed cylinder with reinforcement at 45° to axis; (B) cylinder under tension; (C) cylinder under internal pressure; (D) cylinder under internal pressure plus tension. From Whitney and Halpin (1968).

proaches to shrinkage and drying stress by the New Zealand group (Barber and Meylan 1964; Harris and Meylan 1965; Meylan 1968) are taking into account the problems raised by cell-wall anisotropy.

The fact that many unanswered questions about a cell-wall model with complete shear restraint remain does not in any way diminish from its importance as an advance in our understanding of the mechanical behavior of wood. Neither do the reservations as to its accuracy imply that the single fiber model is more correct. For various situations, one model or another might represent the physical picture more precisely, as will be shown.

THE "TWO-WALL" MODEL AND ITS COMBINATIONS

It seems evident that improvement in models for cell-wall mechanics can be made

in several ways, and the work of Schniewind and Barrett should catalyze more activity in this regard. In this section we introduce an innovation in the method of computing overall strains and the stresses in the various cell-wall layers.

There is no inherent reason why radial and tangential walls must undergo equal transverse strains in wood, as has been assumed by Mark, Cave, and Schniewind and Barrett. The physical situation is such that radial wall segments of adjacent cells can act in concert, as can adjacent tangential wall segments in many species, but that in general, radial and tangential pairs do not act in concert with each other. Since such wall pairs are able to experience different circumferential strains, it is not necessary to specify a zero stress resultant over all of the layers for the circumferential direction, as has been done in all of the previous analyses. It seems more appropriate, at least in the case of coniferous woods, to require an equal circumferential strain for all tangential wall layers and a different equal circumferential strain for all radial wall layers. These two strains would have to be such that the two stress resultants over the layers in the two walls would each be zero for the circumferential direction.

The mathematical expression of this concept can most easily be understood by comparison with the one-wall analysis with complete shear restraint. Eight distinct layers were treated: radial and tangential portions of $M + P$, S1, S2 and S3, although no distinction was made in the earlier analysis between the radial and tangential portions of the first two layers. Equal longitudinal and circumferential strains were assumed to occur in all eight layers. The magnitudes of these two strains were found using the composite elastic properties from the two conditions that the net axial stress be in equilibrium with the axial load, and that the net circumferential stress be zero. In the two-wall analysis, the eight layers are divided into four radial layers, the radial wall, and four tangential layers, the tangential wall. Three independent strains are allowed: a longitudinal strain equal in all eight layers (i.e., in both walls), a circumferential strain in the radial wall, and a different circumferential strain in the tangential wall. These are determined using the composite elastic constants of the radial wall and of the tangential wall from the conditions that the net axial stress be in equilibrium with the axial load, and that the net circumferential stress be zero in both the radial and tangential wall.

For cases in which single fiber assumptions form the basis for calculating composite elastic constants of either a one- or two-wall model, shear strains will generally be required to keep the fiber free of torque. For a one-wall model the single shear strain is determined by requiring the net twisting moment to be zero. For a two-wall model the same condition is sufficient because strain compatibility seems to require equal shear strains in both radial and tangential walls.

The two-wall analysis has been used in all subsequent calculations in this paper. We will also use the refined technique developed by Gillis (1970) for calculating the elastic properties of the individual layers. We believe that this technique offers a substantial improvement in accuracy over the previously employed techniques, which have been based on work by Hill (1965) and Greszczuk (1964), at least in situations where the microfibrils can be treated as being parallel within each layer (or each ply in the case of S1). However, when there is substantial dispersion in the orientations within each layer, the technique of Cave (1968) is likely to be superior. The earlier elastic analysis treated each layer as a side-by-side arrangement of cellulosic microfibrils and strips of matrix connected in series. The revised elastic analysis more realistically treats the microfibrils as being imbedded within the matrix, i.e., completely surrounded by matrix material. This allows a more detailed geometrical description to be used and takes fuller account of the anisotropy of the microfibrils.

The modifications introduced in the stress

TABLE 1. *Microfibril angles and area percentages of the various cell-wall layers in the tracheids originally tested by Mark (1967, Ch. 2, 10), as subdivided by different authors for use in their calculations*

Layer	Filament winding angle	Area, division, % version 1 Mark (1967)	Area, division, % version 2 Schniewind and Barrett (1969)	Area, division, % version 3 Present work
Radial wall				
$M + P$	90°	11.169	11.2	7.40
S1	±80°	17.520	17.5	11.84
S2	36°	30.688	44.1	45.88
S3	64°	6.101	8.8	8.88
Tangential wall				
$M + P$	90°	Note 1	Note 1	2.60
S1	±80°	Note 1	Note 1	4.94
S2	20°	11.166	16.1	16.12
S3	30°	1.649	2.4	2.34
Incomplete cells and fragments				
	90°	21.707	Note 2	Note 3

1. No differentiation between radial and tangential wall segments in $M + P$ and S1 by these authors.
2. Redistributed proportionately into S2 and S3.
3. Not considered; percentages in other layers determined from original measurements of Mark (1965, p. 53).

analysis are illustrated in the following way. The first two columns of Table 1 show the description of the average properties of cells in a microscopic specimen tested by Mark (1967). These characteristics were used by him in his original analysis. The next column of the table gives the values used by Schniewind and Barrett to represent these average properties. Since their analysis is for complete shear restraint, they assumed a test environment in which each cell is completely surrounded by other identical cells, and did not account for effects due to the incomplete cells and fragments actually present in Mark's specimen; they reapportioned the fractional area attributed to these fragments among the other layers. In the last column of the table are shown Mark's original data (for thesis preparation [1965]) for the area fractions in the layers differentiated for the first time with respect to the portions of $M + P$ and S1 assigned to radial and tangential walls. This additional information is of course necessary in a two-wall analysis. These three sets of characteristics will hereafter be referred to as versions 1, 2, and 3 of Mark's cells.

Columns 1 and 2 of Table 2 show the results of applying the Schniewind and Barrett analysis to versions 2 and 3 of Mark's cells. Only insignificant differences occur in the layer stresses. In column 3 of the table are the results from applying the two-wall analysis to the version 3 cell. Again only minor stress changes occur, except for some moderate changes in S1. The last column of the table shows the stresses obtained by further including the revised procedure for calculating elastic properties of the composite layers. Here it can be seen that significant changes appear in the transverse and shear stresses, particularly in S1, where the increase in transverse stress is approximately 65% compared with the results of the other three analyses. This pattern may be expected from the results of Table 3, which shows that the layer transverse Young's modulus E_β has been changed from 400 to 700 kg/mm^2, with a substantial increase also in the shear modulus $G_{\alpha\beta}$ as a result of the revision in method of calculat-

TABLE 2. *Stresses calculated by several different analyses for the layers of the cell of Table 1*

	Schniewind and Barrett results* on version 2			Schniewind and Barrett results on version 3			Two-wall analysis results on version 3			Two-wall analysis with revised† elastic constants on version 3		
	σ_α/σ_x	σ_β/σ_x	$\tau_{\alpha\beta}/\sigma_x$	σ_α/σ_x	σ_β/σ_x	$\tau_{\alpha\beta}/\sigma_x$	σ_α/σ_x	σ_β/σ_x	$\tau_{\alpha\beta}/\sigma_x$	σ_α/σ_x	σ_β/σ_x	$\tau_{\alpha\beta}/\sigma_x$
Radial wall												
$M+P$	−0.279	0.090	0	−0.289	0.089	0	−0.304	0.088	0	−0.276	0.138	0
S1	−1.256	0.160	±0.031	−1.304	0.157	±0.031	−1.370	0.157	±0.031	−1.258	0.264	±0.040
S2	1.682	0.029	0.086	1.642	0.026	0.086	1.621	0.024	0.087	1.543	0.035	0.111
S3	−0.493	0.126	0.071	−0.540	0.123	0.071	−0.594	0.122	0.072	−0.531	0.204	0.092
Tangential wall												
$M+P$	−0.279	0.090	0	−0.289	0.089	0	−0.233	0.091	0	−0.203	0.141	0
S1	−1.256	0.160	±0.031	−1.304	0.157	±0.031	−1.050	0.161	±0.029	−0.927	0.269	±0.037
S2	2.757	−0.019	0.058	2.720	−0.021	0.060	2.758	−0.008	0.055	2.613	−0.019	0.069
S3	2.131	0.009	0.078	2.092	0.006	0.078	2.164	0.018	0.074	2.061	0.026	0.094

Explanation of column headings:

σ_x = externally applied tensile stress in fiber direction

σ_α = internal stress in layer parallel to microfibrils

σ_β = internal stress in layer perpendicular to microfibrils

$\tau_{\alpha\beta}$ = internal shear stress in the plane of the layer

* From Table 2, Schniewind & Barrett (1969)

† Gillis (1970)

TABLE 3. *Constituent and layer elastic constants used in calculations for Table 2*

	Young's modulus ∥ to microfibrils E_α	Young's modulus ⊥ to microfibrils E_β	Shear modulus of rigidity $G_{\alpha\beta}$	Poisson ratio $\nu_{\alpha\beta}$	Poisson ratio $\nu_{\beta\alpha}$
Matrix	204.	204.	78.5	0.3	0.3
Cellulose	13700.	2770.	449.	0.1	0.02
Series analysis (Mark 1967, pp. 233–234)					
Layer with 10.1% cellulose	1567.	225.	85.6	0.28	0.04
Layers with 53.1% cellulose	7370.	401.	139.7	0.19	0.01
Two-wall analysis with elastic constants calculated according to Gillis (1970)					
Layer with 10.1% cellulose	1570.	360.	104.8	0.22	0.05
Layers with 53.1% cellulose	7372.	699.	189.6	0.15	0.01

ing the elastic constants for the two-wall analysis in the last set of columns in Table 2. Note that there is no change of significance in the layer axial modulus of elasticity E_α.

SOME HYPOTHETICAL WOOD FIBERS

Schniewind (1970) has used the cell-wall model with complete shear restraint that he and Barrett developed to examine a series of hypothetical cells having layer filament winding angles, etc. that might represent a spectrum of the fibers occurring in wood. Accordingly, he has labeled these hypothetical cells as "Springwood," "Transition 1," "Transition 2," "Transition 3," and "Summerwood" (See Table 4).

The concept of examining a range of hypothetical cell types can be very instructive in understanding wood and fiber mechanics, and we have also examined a series of such cells. Some of our results are presented herein. We have reservations concerning the appropriateness of the parameters selected by Schniewind, because it seems to us that conclusions regarding behavior of wood should be drawn from hypothetical cases that represent as closely as possible the cells we observe in anatomical study. In some instances Schniewind's hypothetical cells seem unrealistic. As examples:

a. An S3 layer with twice the area of the S2 layer is shown in his "springwood"; real springwood fibers are characterized by a very thin S3 layer; and an S3 equalling, much less exceeding, S2 in area is unknown in any type of wood fiber.

b. In all five hypothetical cell types, S3 exceeds S1 in area; actually the reverse is true in real cells.

c. The $M + P$ fractions given are much lower, for all but the "springwood" type, than would normally be the case.

d. Transition cell #2, which purports to approximate the compression wood case, would have to be adjusted to eliminate S3 (since that layer is absent in compression wood) and at least triple the area for S1 (since S1 is exceedingly thick in compression wood). See for example Côté et al. (1968).

e. Three of the five cell types show S2 as occupying 80% of the cross-sectional area. Only in unusually thick-walled summerwood is such a proportion to be found naturally. When one realizes that $M + P$ occupies 10 to 12% of normal wood solid substance Mark (1967, p. 99), there would be too little allowance for a normal S1 or S3 if S2 were to be 80%.

TABLE 4. *Characteristics of hypothetical fibers used to obtain the results shown in Table 5*

	$M+P$		S1		S2		S3	
	Area fraction	Helical angle	Area fraction	Helical angle	Area fraction	Helical angle	Area fraction	Helical angle
Hypothetical cells of Schniewind (1970)								
"Springwood"	0.1	90°	0.3	80°	0.2	40°	0.4	70°
Transition 1	0.0625	90°	0.1875	80°	0.5	40°	0.25	70°
Transition 2	0.025	90°	0.075	80°	0.8	40°	0.1	70°
Transition 3	0.025	90°	0.075	80°	0.8	25°	0.1	70°
"Summerwood"	0.025	90°	0.075	80°	0.8	10°	0.1	70°
Hypothetical cells of this study								
SPR 1	0.15	90°	0.3	80°	0.4	40°	0.15	70°
SPR 2	0.13	90°	0.245	80°	0.5	40°	0.125	70°
SPR 3	0.11	90°	0.18	80°	0.6	30°	0.11	70°
"Compression wood"	0.07	90°	0.28	80°	0.65	40°	0.0	70°
SUM 1	0.09	90°	0.13	80°	0.7	25°	0.08	70°
SUM 2	0.07	90°	0.08	80°	0.8	10°	0.05	70°

We offer in Table 4 a set of hypothetical cells SPR 1, SPR 2 and SPR 3 that we feel more adequately represent various fibers that might occur in earlywood, and SUM 1 and SUM 2 for corresponding latewood. We have also included in the table a compression wood hypothetical cell type with the typical large S2 angle, thick S1 layer and absent S3 that are all characteristic of compression wood.

In all hypothetical cells, the proportions of matrix and framework in each layer are exactly as given in "Cell wall mechanics of tracheids," p. 114 (Mark 1967), viz.

	MATRIX %	FRAMEWORK %
$M+P$	89.9	10.1
S1, S2 and S3	46.9	53.1

A study of Table 5 reveals that the tensile load is supported mainly by the most nearly axial microfibrils, viz., those in the S2 layer. As S2 is either increased in thickness or aligned more axially, the layer stress σ_α in the microfibril direction is reduced and, as a consequence, the oppositely signed (compressive) directional stresses in the other layers are also reduced. This stress reduction is general since the layer stresses σ_β for the direction normal to the microfibrils (transverse stresses) are correspondingly reduced.

We point out that the largest transverse stress occurs in the S1 layer in every calculation made by us and by Schniewind (1970). Since the experimental evidence indicates that failure generally initiates in the S1 layer or at the S1-S2 boundary, we believe that some critical transverse stress is as likely to be an appropriate failure criterion as some of the other criteria that have been suggested by Mark (1967) and Schniewind and Barrett (1969).

EXPERIMENTS ON ISOLATED FIBERS

We have conducted some recent experiments to examine one of the consequences of the single fiber model. Dependent on the cell dimensions, and modeling a tracheid as a thin-walled hollow cylinder, the shear strain calculations of Mark (1967, Ch. 10) showed that the angle of twist of one end of a fiber could easily be more than 400° with respect to the other end when the fiber is stressed axially. We had not previously verified this twisting experimentally and are not aware of such an experiment's having been conducted elsewhere.

Matchstick-size pieces of Virginia pine (*Pinus virginiana* Mill.) were selected from the fifteenth ring and macerated in equal parts of glacial acetic acid and hydrogen peroxide. After washing and conditioning

TABLE 5. *Layer stresses in hypothetical wood fibers, using the "Two-Wall" analysis with revised* calculation of elastic constants for the layers, with framework and matrix elastic constants taken from Mark (1967)*

Values in parentheses are for a cell wall model with complete shear restraint as per Schniewind (1970); all calculations assume $M + P$ to be 10.1% framework and S1, S2, S3 to be 53.1% framework

	$M+P$			S1		
	σ_α/σ_x†	σ_β/σ_x	$\tau_{\alpha\beta}/\sigma_x$	σ_α/σ_x	σ_β/σ_x	$\pm\tau_{\alpha\beta}/\sigma_x$
Hypothetical cells of Schniewind (1970)						
"Springwood"	-0.181(-.24)	0.353(.28)	0.0(0.0)	-0.847(-1.08)	0.667(.49)	0.076(.07)
Transition 1	-0.302(-.35)	0.240(.17)	0.0(0.0)	-1.384(-1.59)	0.456(.29)	0.061(.05)
Transition 2	-0.613(-.71)	0.212(.14)	0.0(0.0)	-2.787(-3.22)	0.409(.25)	0.071(.06)
Transition 3	-0.222(-.25)	0.087(.05)	0.0(0.0)	-1.009(-1.14)	0.167(.10)	0.028(.02)
"Summerwood"	-0.046(-.05)	0.061(.04)	0.0(0.0)	-0.212(- .24)	0.116(.07)	0.014(.01)
Hypothetical cells of this study						
SPR 1	-0.242	0.265	0.0	-1.115	0.503	0.062
SPR 2	-0.299	0.240	0.0	-1.369	0.456	0.060
SPR 3	-0.210	0.134	0.0	-0.960	0.255	0.036
"Compression wood"	-0.352	0.209	0.0	-1.610	0.398	0.057
SUM 1	-0.181	0.097	0.0	-0.825	0.186	0.027
SUM 2	-0.046	0.062	0.0	-0.214	0.117	0.014

	S2			S3		
	σ_α/σ_x	σ_β/σ_x	$\tau_{\alpha\beta}/\sigma_x$	σ_α/σ_x	σ_β/σ_x	$\tau_{\alpha\beta}/\sigma_x$
Hypothetical cells of Schniewind (1970)						
"Springwood"	3.902(5.00)	0.280(.22)	0.219(.21)	-0.106(- .13)	0.607(.45)	0.143(.13)
Transition 1	2.402(2.73)	0.147(.10)	0.174(.15)	-0.794(- .92)	0.408(.26)	0.114(.10)
Transition 2	1.656(1.79)	0.047(.03)	0.205(.17)	-2.094(-2.44)	0.353(.22)	0.134(.11)
Transition 3	1.441(1.47)	-0.033(-.02)	0.062(.05)	-0.740(- .86)	0.145(.08)	0.052(.04)
"Summerwood"	1.258(1.27)	-0.004(.00)	0.014(.01)	-0.076(- .10)	0.105(.06)	0.026(.02)
Hypothetical cells of this study						
SPR 1	2.785	0.185	0.180	-0.507	0.453	0.117
SPR 2	2.408	0.148	0.174	-0.780	0.408	0.114
SPR 3	1.944	0.019	0.091	-0.610	0.227	0.068
"Compression wood"	1.969	0.107	0.165	——	——	——
SUM 1	1.617	-0.014	0.062	-0.557	0.164	0.052
SUM 2	1.216	-0.004	0.014	-0.078	0.105	0.026

* Gillis (1970)
† Explanation of column headings given in Table 2

to 72 F, 50% RH, the tracheids were spread out under a dissecting microscope. A selection was made for the straightest fibers and these were bonded at one end to either a paper triangle or a strain gage mounted on the end of a 3⁄32-inch-diameter wood rod with an epoxy bonding cement. This rod was subsequently pin-connected to a simple wood post mounted on plywood so that it could swivel stiffly.

Under the end of the rod that held the fiber and its paper or strain gage holder, a piece of polar graph paper was placed so that it was centered under the fiber. An acrylic capsule filled nearly to the top with a clear epoxy embedding resin was positioned under the fiber. Attached to the base of this capsule and passing directly across the center of the base was a needle, which we aligned at 0° on the graph paper.

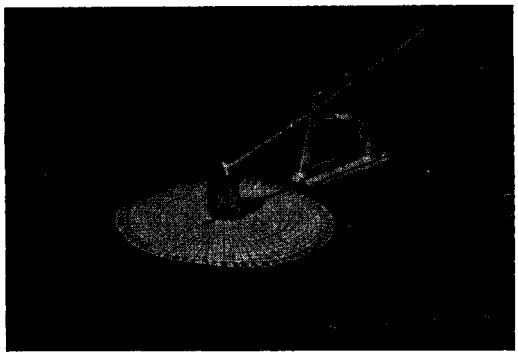

FIG. 6. Apparatus for measuring twist of a single fiber under tension. In testing, the rod is swiveled about a pin on the front post, elevating the capsule. The rod is pressed into a notch on the back post to maintain the suspension in air.

FIG. 7. Capsule and needle suspended on a fiber above polar graph paper to measure angular rotation.

The rod was then swiveled so that the fiber dipped into the resin slightly, perhaps 1 mm, and the entire apparatus, shown in Fig. 6, was placed in an oven at 50 C to cure the resin.

After cure, the test is conducted by swiveling the wood rod so as to lift the capsule and needle with the fiber, and a view of such a test, with the capsule elevated, is shown in Fig. 7. The amount of rotation we have observed has been variable, because it depends on the free span length of the fiber between the capsule and the paper triangle or strain gage as well as other factors, but we have recorded initial rotations of from 40° to 330°. Since the predominant helix in a tracheid is the Z helix of S2, one would expect the rotations to be counterclockwise (as they are in the analogous tubes of Fig. 5), and this expectation is confirmed. We have performed six successful tests on single fibers. After each test, the free span length is measured and the capsule plus needle is weighed. We also attempt to determine the S2 angle and the cross-sectional area, but have not been entirely successful. Measurement of fiber elongation was accomplished on the last test by using a strain gage as a visual micrometer (see Figs. 8a and 8b). The spacing of the bars in the strain gage is known; thus they can be used to measure the length of the fiber span before and after test by direct proportion.

A summary of the results of these tests is given in Table 6. The one measurement of fiber strain given in Table 6 seems rather high, and it may not be entirely elastic strain. On the photographs, the initial free length of the slack fiber (Fig. 8a) was calculated to be 1.21 mm. In the stretched state under tension (Fig. 8b), it measures 1.30 mm. As an independent check, the fiber was severed after test at the capsule and at the gage end, and the cut length was measured on the microscope with a filar eyepiece micrometer. This measurement gave 1.24 mm. We are not confident enough of our measurements to know if the 0.03 mm difference between this and the original length before test is a real one.

We have also embedded the tracheid used for test #7 and resectioned it transversely, in order to measure cross-sectional area by the cutout-weighing method (Mark 1967, p. 52). This area, 0.0004678 mm^2, indicates that the applied tensile stress was 6.95 kg/mm^2. The cross-section is shown in Fig. 9.

We were also interested in the time-dependent behavior of the twist, and allowed two of the fibers, #4 and #7, to hang for 10 min, during which time fiber #4 continued to rotate extensively, and went from the initial twist of 330° to 480° at the end of this period. By contrast, fiber #7 in-

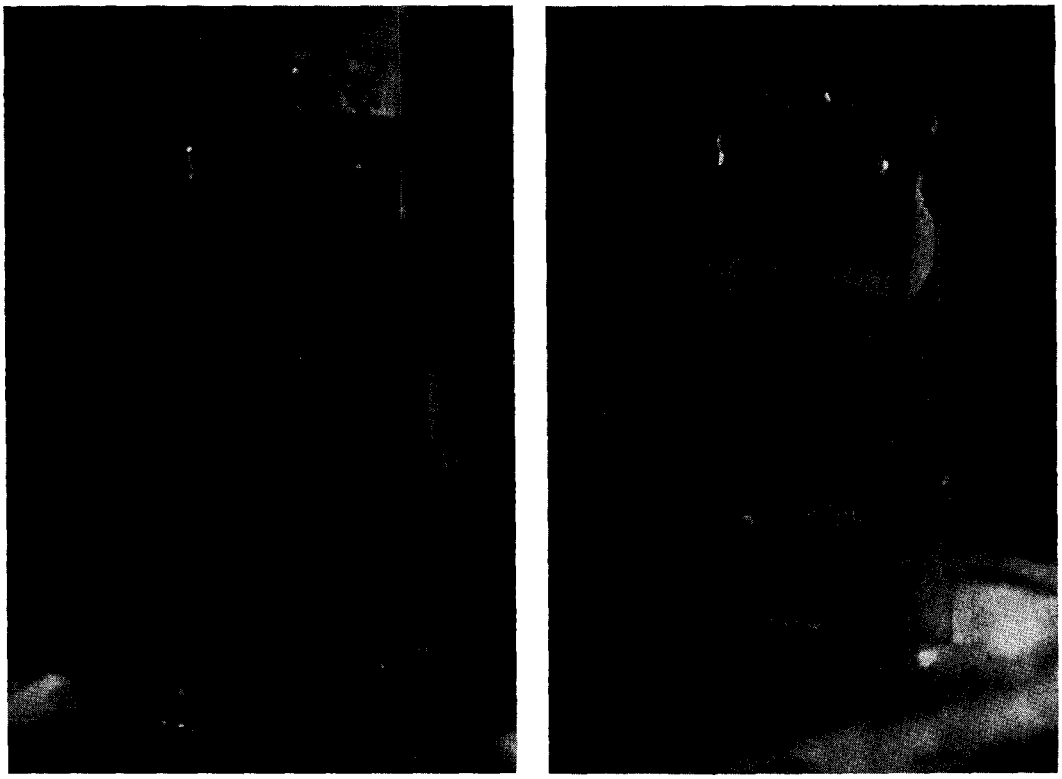

FIG. 8. Greatly enlarged view of the strain gage and tracheid mounted on the end of a rod for test #7. The fiber is shown extending from the end of the strain gage to the surface of the hardened resin in the capsule.

a. Condition before test, with fiber slack.
b. Condition during test with fiber extended; free span length measured in small increments along fiber shows a total length increase of 7.4%.

creased by only 5° in the 10-min time (215° to 220°). We ran one longer test, allowing fiber #3 to hang for 24 hr. During this time, its twist angle increased from the initial 250° to 515°.

In Table 6, no test #2 is shown. This is because we mistakenly tested two fibers together that had not quite come apart during pulping. However, the results are interesting. In spite of a long free span length (2.91 mm), the initial rotation was only 50°, which indicates that the fibers are restraining each other as would be expected. The capsule and needle weighed 2.86 grams in this case.

From these experiments, it appears that the single fiber model is one that can reasonably describe the mechanical behavior for isolated tracheids and similar lignocellulosic fibers. The rotations predicted by the single fiber model, which might offhand seem too large, are actually exceeded in the case of these isolated tracheids. One must allow for the fact that part of the stiffening matrix has been removed in the maceration process, of course. We are quite confident also that the observed rotations are due exclusively to fiber twisting. The measurements would be invalid if there were camera movements or strain gage deflection, but no change in camera position was allowed, and there was no evidence of the latter problem's existing.

SUMMARY AND CONCLUSIONS

Consideration of the various models that have been offered to explain the mechanical behavior of wood cell walls suggests that

TABLE 6. *Rotation tests of single fibers (tracheids of pine) under tension*

Specimen number	Initial capsule rotation	Free span length	S2 angle est.	Applied load	Fiber elongation
1	165° ccw	2.57 mm	18.5°	2.80 gm	——
3	250° ccw	1.55 mm	——	2.70 gm	——
4	330° ccw	2.31 mm	18.9°	2.95 gm	——
5	200° ccw	1.66 mm	18.2°	3.10 gm	——
6	40° ccw	0.65 mm	——	3.05 gm	——
7	215° ccw	1.24 mm	18.7°	3.25 gm	7.4%

some of the assumptions made in each case are not justified. Complete shear restraint (Cave 1968; Schniewind and Barrett 1969) is practically unattainable within the cells of wood; however, an assumption that shear restraint occurs only within the S1 layer (Mark 1967) allows far more shear strain in the total wall than is possible within wood generally. Of the two approaches, an assumption of complete shear restraint is closer to physical reality, and a means of improving this approach is offered wherein the radial and tangential wall segments may undergo different circumferential strains. We call this the "two-wall" method; combined with an improved technique of Gillis (1970) for determining the elastic constants of each layer and the resultant compliances of the laminated wall, the method yields substantial changes in the stress distribution pattern within the walls of the cells analyzed previously by Mark and by Schniewind and Barrett. The most dramatic change is shown in the S1 layer, where transverse stresses over 65% greater than those previously calculated are shown.

A series of hypothetical cells representing springwood, summerwood, and compression wood, which we feel are more realistic than those selected by Schniewind (1970), are examined by the improved two-wall method. We have also performed this analysis on Schniewind's hypothetical cells. In all cases, stresses in the direction normal to the microfibrils are at a maximum in the S1 layer. This suggests that a third possibility exists to explain the general experimental evidence that failure initiates in S1 or at the S1 boundary—transverse stress causing ruptures within the matrix or framework constituents or both may be initiating a stress redistribution. This is in contrast to the previous evidence offered to support concepts of a shearing mechanism (Mark 1967) or buckling instability of microfibrils (Schniewind and Barrett 1969) in S1.

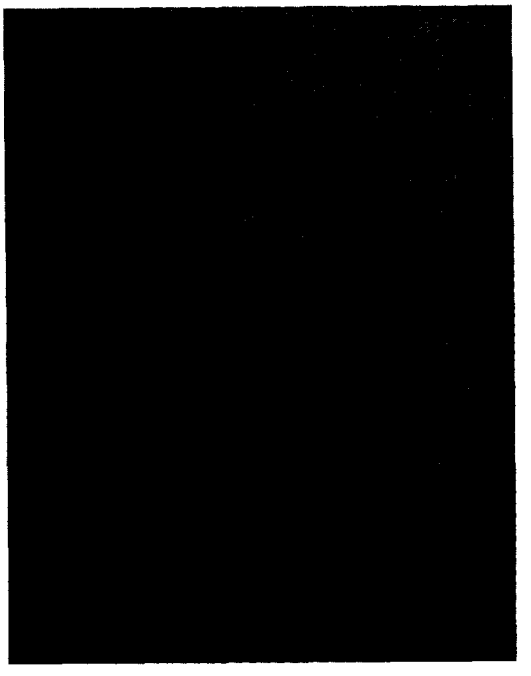

FIG. 9. Magnified cross section of tracheid shown in Fig. 8 after testing. Undissolved remnants of the middle lamella remain on the outer surface.

We believe, on the basis of the experiments described in this paper, that the "single fiber" model with shear restraint only in S1 that was developed by Mark (1967) represents the mechanical behavior of independent fibers rather well. In the future, we might impose numerical values on such parameters as shear strain or ratio of shear strain to axial extension to compare the behavior of our models with these fibers more closely. The various cell-wall models that have been offered should permit improved calculations for stress analysis of wood, fibers and wood fiber structures including paper to be made, perhaps by combining some features of various models.

ACKNOWLEDGMENT

Funds for this research were made available under the provision of the McIntire-Stennis Cooperative Forestry Research Program of the U. S. Department of Agriculture. The authors are indebted to this agency and the Kentucky Agricultural Experiment Station for their support on this project. The numerical analysis was completed on the facilities at the University of Kentucky Computing Center. The authors would like to express their appreciation to Dr. J. C. Halpin of the Air Force Materials Laboratory for providing technical documents and other assistance, to Mr. J. D. Webb and Mrs. H. B. Smith for their cheerful perserverance and hard work in the delicate laboratory work that was necessary to accomplish the tests that have been described, to Yale University Press for permission to reproduce Figs. 1 and 2, to Technomic Publishing Co., for Figs. 3 and 5, and to the American Society for Mechanical Engineers for Fig. 4.

REFERENCES

Ashton, J. E., J. C. Halpin, and P. H. Petit. 1969. Primer on composite materials: Analysis. Technomic Pub. Co., Stamford, Conn. 124 pp.

Balashov, V., R. D. Preston, G. W. Ripley, and L. C. Spark. 1957. Structure and mechanical properties of vegetable fibres. I. The influence of strain on the orientation of cellulose microfibrils in sisal leaf fibre. Proc. Roy. Soc. (London) B, **146**: 460–468.

Barber, N. F., and B. A. Meylan. 1964. The anisotropic shrinkage of wood. A theoretical model. Holzforsch., **18**(5): 146–156.

Cave, I. D. 1968. The anisotropic elasticity of the plant cell wall. Wood Sci. Tech., **2**(4): 268–278.

———. 1969. The longitudinal Young's modulus of *Pinus radiata*. Wood Sci. Tech., **3**: 40–48.

Côté, W. A., Jr., A. C. Day, and T. E. Timell. 1968. Studies on compression wood—Part VII: Distribution of lignin in normal and compression wood of tamarack [*Larix laricina* (Du Roi) K. Koch] Wood Sci. Tech., **2**: 13–37.

Cowdrey, D. R., and R. D. Preston. 1966. Elasticity and microfibrillar angle in the wood of Sitka spruce. Proc. Roy. Soc. (London) B, **166**: 245–272.

Davies, G. W. 1968. Microscopic observations of wood fracture. Holzforsch., **22**: 177–181.

Esau, K. 1960. Anatomy of seed plants. John Wiley Inc., New York,. 376 pp.

Gillis, P. P. 1970. Elastic moduli for plane stress analyses of unidirectional composites with anisotropic rectangular reinforcement. Fibre Sci. Tech. **2**: 193–210.

Greszczuk, L. B. 1964. Elastic constants and analysis methods for filament wound shell structures. Douglas Aircraft Missile and Space Systems Div., Rept. SM-45849.

Grozdits, G. A. and G. Ifju. 1969. Development of tensile strength and related properties in differentiating coniferous xylem. Wood Sci., **1**(3): 137–147.

Harris, J. M., and B. A. Meylan. 1965. The influence of microfibril angle on longitudinal and tangential shrinkage in *Pinus radiata*. Holzforsch., **19**(5): 144–153.

Hearle, J. W. S. 1963. The fine structure of fibers and crystalline polymers. III. Interpretation of mechanical properties of fibers. J. Appl. Polymer Sci., **7**: 1207–1223.

Hill, R. 1965. Theory of mechanical properties of fibre strengthened materials. III. Self-consistent model. J. Mech. Phys. Solids, **13**: 189–198.

Keith, C. T. and W. A. Côté, Jr. 1968. Microscopic characterization of slip lines and compression failures in wood cell walls. Forest Prod. J., **18**(3): 67–74.

Kórán, Z. 1967. Electron microscopy of radial tracheid surfaces of black spruce separated by tensile failure at various temperatures. TAPPI, **50**: 60–67.

Mark, R. E. 1965. Treatise on the tensile strength of tracheids. D. For. Dissert., Yale University.

———. 1967. Cell wall mechanics of tracheids, Yale University Press, 310 pp.

Meylan, B. A. 1968. Cause of high longitudinal shrinkage in wood. *Forest Prod. J.*, **18**(4): 75–78.

REISSNER, E. AND Y. STAVSKY. 1961. Bending and stretching of certain types of heterogeneous aeolotropic elastic plates. J. Appl. Mech., **28**: 402–408.

SCHNIEWIND, A. P. 1970. Elastic behavior of the wood fiber. *In* B. A. Jayne (ed.), Theory and design of wood and fiber composite materials, Univ. Wash., Seattle.

——— AND J. D. BARRETT. 1969. Cell wall model with complete shear restraint. Wood & Fiber, **1**(3): 205–214.

SMITH, C. B. 1953. Some new types of orthotropic plates laminated of orthotropic material. J. Appl. Mech., **20**: 286–288.

WHITNEY, J. M. 1969. Bending-extensional coupling in laminated plates under transverse loading. J. Composite Materials, **3**: 20–28.

——— AND J. C. HALPIN. 1968. Analysis of laminated anisotropic tubes under combined loading. J. Composite Materials, **2**(3): 360–367.

——— AND A. W. LEISSA. 1969. Analysis of heterogeneous anisotropic plates. J. Appl. Mechanics, **36**: 261–266.

Wood and Fiber publishes abstracts of articles from appropriate foreign journals. These abstracts are spaced throughout the journal at the ends of articles. In addition, there is a separate section of them in this issue, near the end of the journal. Francis C. Beall, of Pennsylvania State University, is chairman of the committee responsible for these abstracts. Other members of the committee are: R. M. Kellogg, R. T. Lin, R. L. Ethington, Ali Moslemi, J. D. Wellons, E. G. King, D. D. Nicholas, J. D. Snodgrass, and Joe Yao.